Density Functional Theory Investigations of the Forbidden Double Insertion of Diazomethane into Zr−C Bonds of $Cp_2Zr(CH_3)_2$

P. Jeffrey Hay†

Theoretical Division, Los Alamos National Laboratory, Los Alamos, New Mexico 87545

Received February 3, 2007

The potential energy surfaces involved in the insertion of diazomethane species R_2CN_2 (R = H, Ph) into the $Zr-CH_3$ bonds of $Cp_2Zr(CH_3)_2$ are examined using density functional methods. The first insertion leads to the experimentally observed mono-hydrazonato complex $Cp_2Zr(CH_3)(CH_3-N-N=CPh_2)$, for which the reaction energy is calculated to be −37 kcal/mol. Insertion of a second diazomethane molecule into the remaining Zr−Me bond leads to the bis-hydrazonato complex $Cp_2Zr(CH_3-N-N=CPh_2)_2$, which is calculated to be a stable species with an overall reaction exothermicity of −27 kcal/mol. While the first insertion proceeds with a small activation barrier (2−7 kcal/mol), a more substantial activation barrier (25 kcal/mol) is found for the second insertion, but not sufficiently large to preclude formation of the bis-hydrazonato complex. This formally 20-valence-electron species is hence predicted to be a target for synthesis. The bonding in the bis-hydrazonato complexes shows significant Zr 4d admixture in the MOs involving the four σ donors from the nitrogen ligands. Stabilization strategies for the complexes by varying ligand electronegativity are investigated.

Introduction

The insertion of reactants possessing C=O and C=N linkages into metal−carbon bonds represents one of the more widely studied reactions in organometallic chemistry. The insertion of CO into M−C bonds has been the subject of extensive experimental and theoretical studies as a fundamental step in carbonylation reactions of organometallic complexes.[1] Related insertion reactions involving unsaturated N-donors leading to Zr−N bond formation include alkyl isonitriles and diazomethane derivatives.[2]

In the area of group 4 chemistry, the reaction of CO with $Cp_2Zr(CH_3)_2$ forms $Cp_2Zr(CH_3)(CH_3CO)$,[3] while reaction with $(C_5Me_5)_2Zr(CH_3)_2$ proceeds successively through the mono-acetyl complex to form the *cis*-$(C_5Me_5)_2Zr$(enediolate) complex.[4] The features of the CO insertion into the M−C bonds of $Cp_2M(CH_3)_2$ for M = Ti and Zr were mapped out initially by Lauher and Hoffmann[5] and by Tatsumi et al.[6] in the formation of acyl complexes $Cp_2M(CH_3)(\eta^2\text{-}CH_3CO)$. Later theoretical studies by Tatsumi et al.[7] and Hoffman et al.[8] studied the mechanisms of the double carbonylation process and examined the differences between actinide and group 4 metals. More recent DFT calculations have studied the potential energy surfaces involved in CO insertion into Zr−C bonds of $Cp_2Zr(CH_3)_2$ as well as dynamical simulations by de Angelis et al.[9,10] Budzelaar studied the CO insertion into the Zr−C bond of Cp_2Zr^+ with regard to copolymerization of CO and C_2H_4.[11]

With regard to reactants containing C=N linkages recent theoretical studies treated insertion of isocyanides into M−C and M−N bonds,[12,13] Experimentally the related insertion reaction of diazomethane derivatives into Zr−C bonds of Cp_2ZrMe_2 to form the hydrazonato complex $Cp_2Zr(CH_3)(CH_3-N-N=CPh_2)$ (**1-Ph**) was first demonstrated experimentally by Gambarotta et al.[14,15]

$$Cp_2Zr(CH_3)_2 + Ph_2C=N=N \rightarrow Cp_2Zr(CH_3)(CH_3-N-N=CPh_2) \quad (1)$$

using both Cp_2ZrMe_2 and $Cp_2ZrMeCl$ as starting points. A second insertion reaction to form the bis-hydrazonato species **3-Ph** is not observed. These observations are consistent with

$$Cp_2Zr(CH_3)(CH_3-N-N=CPh_2) + Ph_2C=N=N \rightarrow Cp_2Zr(CH_3-N-N=CPh_2)_2 \quad (2)$$

the 18-electron rule for transition metal complexes if one treats the η^2-hydrazonato ligands (hyd) in the conventional manner as four-electron donors. The species **1-Ph** would have 18 valence electrons arising from four electrons from the hyd ligand, two from Me, and six each from the Cp ligands. By contrast, the complex **3-Ph** represents a formally 20-valence-electron species.

† E-mail: pjhay@lanl.gov.

(1) Kuhlmann, E. J.; Alexander, J. J. *Coord. Chem. Rev.* **1980**, *33*, 195.
(2) Durfee, L. D.; Rothwell, I. P. *Chem. Rev.* **1988**, *88*, 1059.
(3) Fachinetti, G.; Floriani, C.; Merchetti, F.; Merlino, S. *J. Chem. Soc., Chem. Commun.* **1976**, 572.
(4) Manriquez, J. M.; McAlister, D. R.; Sanner, R. D.; Bercaw, J. E. *J. Am. Chem. Soc.* **1978**, *100*, 2716.
(5) Lauher, J. W.; Hoffmann, R. *J. Am. Chem. Soc.* **1976**, *98*, 1729.
(6) Tatsumi, K.; Nakamura, A.; Hofmann, P.; Stauffert, P.; Hoffmann, R. *J. Am. Chem. Soc.* **1985**, *107*, 4440.
(7) Tatsumi, K.; Nakamura, A.; Hofmann, P.; Hoffmann, R.; Moloy, G. G.; Marks, T. J. *J. Am. Chem. Soc.* **1986**, *108*, 4467.
(8) Hofmann, P.; Stauffer, P.; Frede, M.; Tatsumi, K. *Chem. Ber.* **1989**, *122*.
(9) De Angelis, F.; Sgamellotti, A.; Re, N. *Organometallics* **2000**, *19*, 4904.
(10) De Angelis, F.; Sgamellotti, A.; Re, N. *J. Chem. Soc., Dalton Trans.* **2001**, 1023.
(11) Budzelaar, P. H. M. *Organometallics* **2004**, *23*, 855.
(12) Martins, A. M.; Ascenso, J. R. *Organometallics* **2003**, *22*, 4218.
(13) Martins, A. M.; Ascenso, J. R.; de Azeveda, C. G.; Dias, A. R.; Duarte, M. T.; da Silva, J. F.; Veiros, L. F.; Rodrigues, S. S. *Organometallics* **2003**, *22*, 4218.
(14) Gambarotta, S.; Basso-Bert, M.; Floriani, C.; Guastini, C. *Chem. Commun.* **1982**, 374.
(15) Gambarotta, S.; Floriani, C.; Chiesei-Villa, A.; Guastini, C. *Inorg. Chem.* **1983**, *22*, 2029.

10.1021/om070107w CCC: $37.00
Publication on Web 08/03/2007

In contrast, actinide complexes form both mono- and bis-hydrazonato complexes. Examples such as $Cp^*_2U(Me-N-N=CR_2)(OTf)$ and $Cp^*_2An(Me-N-N=CR_2)_2$ (where An = Th and U) have been synthesized and characterized by Kiplinger and co-workers.[16,17] Several synthetic strategies have been used, among which $Cp^*_2An(CH_3)_2 + Ph_2C=N=N$ have been used as starting points. The electronic properties of bis-hydrazonato U complexes have been explored theoretically in which both 6d and 5f orbitals were found to play an important role in the bonding.[18] Reaction energies for formation of bis-hydrazonato complexes were calculated to be very exothermic (−100 kcal/mol) relative to $Cp_2U(CH_3)_2 + 2\ Ph_2C=N=N$. In this paper we examine the successive insertion reactions of $R_2C=N=N$ into the $Zr-CH_3$ bonds of $Cp_2Zr(CH_3)_2$ where R = H and Ph to form the mono-hydrazonato complex and the as-yet-unobserved bis-hydrazonato species $Cp_2Zr(Me-N-N=CR_2)_2$.

Details of the Calculation

The structures and energies of Zr complexes were determined by geometry optimization with the B3LYP hybrid functional.[19] The optimizations were carried out using the LANL2DZ basis for Zr[20] and 6-31G basis for ligands and a relativistic effective core potential (RECP) for Zr. This basis set, used for nearly all the calculations, will be denoted BS1. Vibrational frequencies were computed at stable points and for transition states to obtain zero-point energy corrections at 0 K and related thermodynamic properties at 298 K. Solvent corrections for toluene were included using the PCM dielectric continuum model with UFF radii. All calculations were carried out using the Gaussian03 suite of programs.[21]

In addition, single-point calculations were performed in a few selected cases with an expanded basis set (BS2) comprised of an uncontracted basis set on Zr with the same Gaussian primitive basis with an added 4f polarization function ($\alpha = 0.3$) and a 6-31 G* basis on the ligands. Results in BS2 were compared using the B3LYP and PBE functional[22] as well as employing conventional MP2 theory. As described in the text, additional calculations were carried out on diphenyl hydrazonato complexes using fluorine substitutents on the phenyl rings (both perfluoro and 4-fluoro cases) in which geometries and resulting energies were obtained in the original BS1 using the B3LYP functional.

The thermochemistry presented in the paper is based on the electronic energies in BS1 including zero-point vibrational contributions at 0 K. The enthalpies ΔH (298 K) and Gibbs free energies ΔG (298 K) are presented in the Supporting Information. The reaction profiles using calculated enthalpies typically differ by about 1 kcal/mol from results using electronic energies. Comparing reaction pathways using Gibbs free energies, by contrast, gives significant differences (a change of 12 kcal/mol compared to reaction enthalpies) if all species are treated as gas-phase molecules due to loss of translational and rotational entropy. For solution-phase reactions of interest in this study, however, one expects the effects of translational and rotational entropy in particular to be mitigated to a significant degree. A recent study of Cp_2Zr-catalyzed hydrosilylation of ethylene by Sakaki et al.[23] pointed out that uncorrected gas-phase Gibbs free energies can overestimate these effects. They also showed that free energy differences computed using only vibrational contributions gave similar results to electronic energies corrected for zero-point energies and were more consistent for solution-phase insertion reactions.

Results

First Insertion Reaction. We consider the reaction pathway for insertion of diazomethane species, CR_2N_2, into the $Zr-CH_3$ bonds of $Cp_2Zr(CH_3)_2$, where R = H and Ph (eq 1). As has been pointed out in the literature previously,[5] there are two possible approaches for the insertion: the central approach between the two Me groups and the lateral approach to the side of one of the Zr−Me bonds. From fragment MO analysis of Cp_2Zr, two of the three frontier orbitals (a_1 and b_2 symmetry) are involved in the Zr−Me bonds, leaving the remaining acceptor orbital (a_1), which has lobes along both the central and lateral approaches.

The calculated reaction pathways for the central and lateral approaches are shown schematically for R = H in Figures 1 and 2, respectively. The corresponding pathways for R = Ph are given in Figure 3. Considering the reaction thermochemistries (see Table 1), we note that the initial insertion to form **1-Ph** (−37.3 kcal/mol) is favored relative to the **2-Ph** isomer (−34.1 kcal/mol). This is consistent with the experimental isolation of **1-Ph** by Gamboratta et al.[15] The same trend is observed in the model species, where the ordering **1-H** < **2-H** is similarly observed.

The structural parameters for the experimentally observed $Cp_2Zr(CH_3)(CH_3-N-N=CPh_2)$ species **1-Ph** are compared with the calculated values for the calculated **1-H** and **1-Ph** complexes in Table 2. Structures are also displayed in Figure 4. In product **1-Ph** a shorter covalent bond is formed between the $Zr-N_1$ bond (2.142 Å calc, 2.103 Å expt) and a longer $Zr-N_2$ bond (2.338 Å calc, 2.283 Å expt) corresponding to the dative interaction.

The reaction path for this first step was explored briefly for the model R = H systems. For the central approach, a slightly bound adduct is formed initially (−0.6 kcal/mol) followed by a small barrier (+2.0 kcal/mol) along the path to form the $Cp_2Zr(CH_3)(CH_3-N-N=CH_2)$ hydrazonato complex **2-H** (Me-out) isomer. The transition state (**lat TST1**) corresponding to lateral approach has a higher barrier (+7.0 kcal/mol), as depicted in Figure 2. Also the transition state ($\mathbf{TST_{12}}$) corresponding to conversion of **2-H** (Me-out) to **1-H** (Me-in) species was identified. The structure (Figure 5) involves twisting the ligand about the Zr−NN axis with a resultant barrier 8.4 kcal/mol higher than **2-H**. We note that earlier theoretical calculations for CO insertion into $Cp_2Zr(CH_3)_2$ favored the lateral approach[9] along which a weakly bound adduct (−1.3 kcal/mol) was found.

Second Insertion Reaction. We now consider the possibility of a second insertion of $R_2C=N=N$ into the remaining Zr−

(16) Kiplinger, J. L.; John, K. D.; Morris, D. E.; Scott, B. L.; Burns, C. J. *Organometallics* **2002**, *21*, 4306.
(17) Morris, D. E.; da Re, R. E.; Jantunen, J. C.; Castro-Rodriguez, I.; Kiplinger, J. L. *Organometallics* **2004**, *23*, 5142.
(18) Hay, P. J. *Faraday Discuss.* **2003**, *124*, 69.
(19) Becke, A. D. *J. Chem. Phys.* **1993**, *98*, 5648.
(20) Hay, P. J.; Wadt, W. R. *J. Chem. Phys.* **1985**, *82*, 299.
(21) Frisch, M. J.; Trucks, G. W.; Schlegel, H. B.; Scuseria, G. E.; Robb, M. A.; Cheeseman, J. R.; Montgomery, J. A., Jr.; Vreven, T.; Kudin, K. N.; Burant, J. C.; Millam, J. M.; Iyengar, S. S.; Tomasi, J.; Barone, V.; Mennucci, B.; Cossi, M.; Scalmani, G.; Rega, N.; Petersson, G. A.; Nakatsuji, H.; Hada, M.; Ehara, M.; Toyota, K.; Fukuda, R.; Hasegawa, J.; Ishida, M.; Nakajima, T.; Honda, Y.; Kitao, O.; Nakai, H.; Klene, M.; Li, X.; Knox, J. E.; Hratchian, H. P.; Cross, J. B.; Adamo, C.; Jaramillo, J.; Gomperts, R.; Stratmann, R. E.; Yazyev, O.; Austin, A. J.; Cammi, R.; Pomelli, C.; Ochterski, J. W.; Ayala, P. Y.; Morokuma, K.; Voth, G. A.; Salvador, P.; Dannenberg, J. J.; Zakrzewski, V. G.; Dapprich, S.; Daniels, A. D.; Strain, M. C.; Farkas, O.; Malick, D. K.; Rabuck, A. D.; Raghavachari, K.; Foresman, J. B.; Ortiz, J. V.; Cui, Q.; Baboul, A. G.; Clifford, S.; Cioslowski, J.; Stefanov, B. B.; Liu, G.; Liashenko, A.; Piskorz, P.; Komaromi, I.; Martin, R. L.; Fox, D. J.; Keith, T.; Al-Laham, M. A.; Peng, C. Y.; Nanayakkara, A.; Challacombe, M.; Gill, P. M. W.; Johnson, B.; Chen, W.; Wong, M. W.; Gonzalez, C.; Pople, J. A. *Gaussian 03*, Revision B.04 ed.; Gaussian, Inc.: Pittsburgh, PA, 2003.
(22) Perdew, J. P.; Burke, K.; Ernzerhof, M. *Phys. Rev. Lett.* **1996**, *77*, 3865.
(23) Sakaki, S.; Takayama, T.; Sumimoto, M.; Sugimoto, M. *J. Am. Chem. Soc.* **2004**, *126*, 3332.

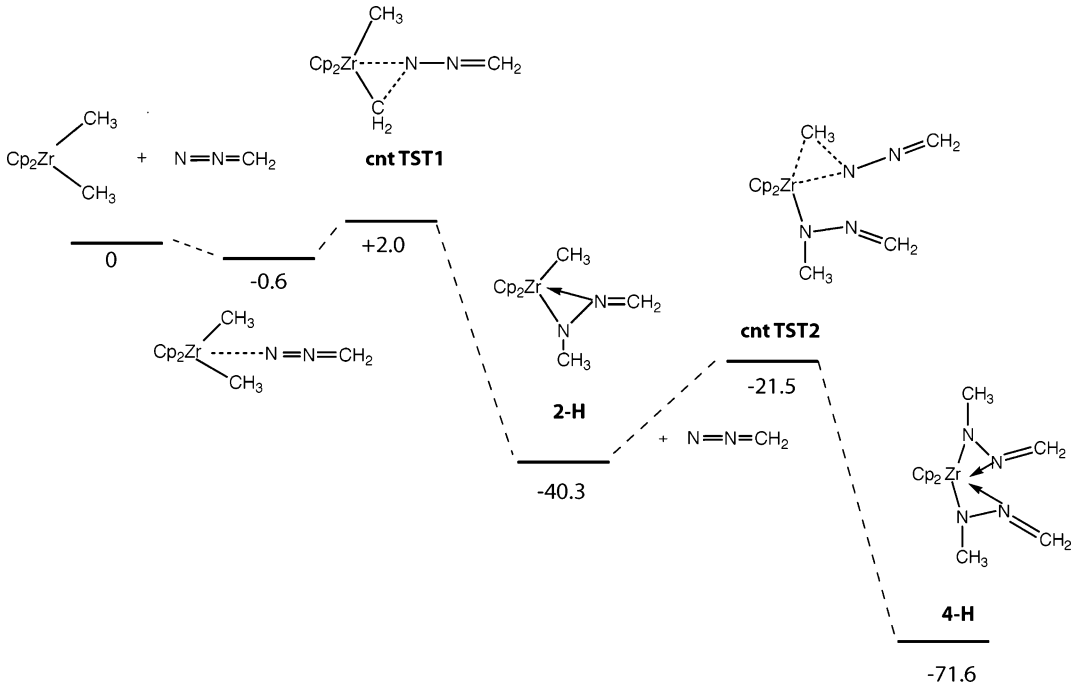

Figure 1. Reaction path of central addition of $H_2C{=}N{=}N$ to Cp_2ZrMe_2. Energies include zero-point corrections.

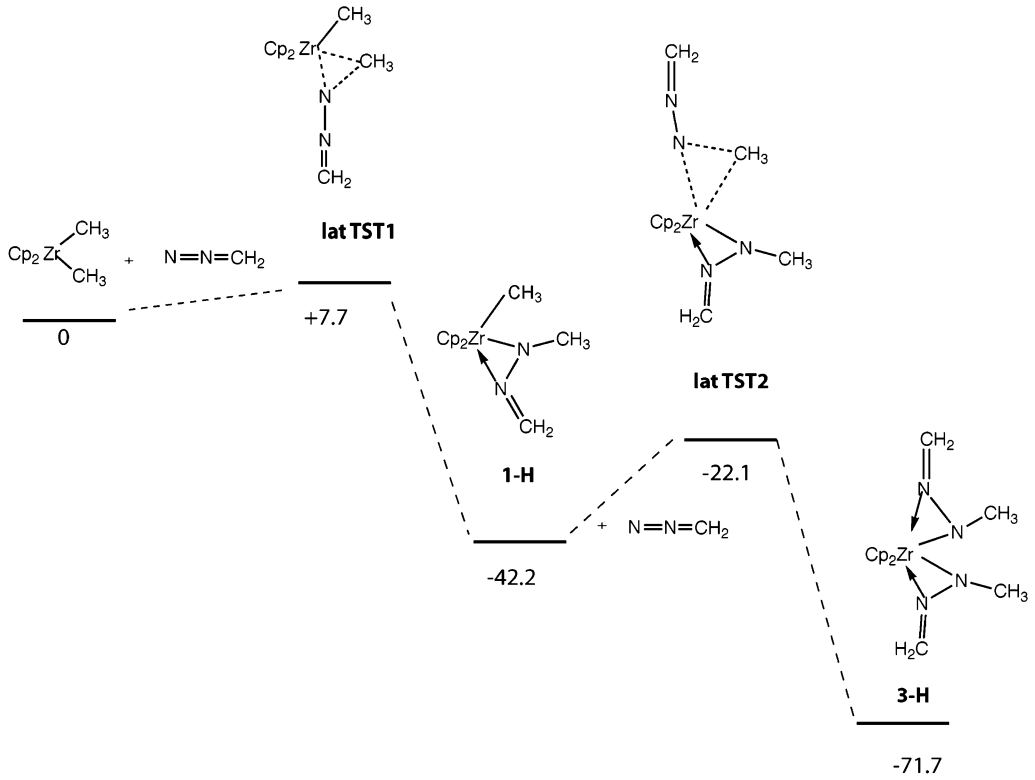

Figure 2. Reaction path of lateral addition of $H_2C{=}N{=}N$ to Cp_2ZrMe_2.

CH_3 bond to form the bis-hydrazonato complexes (eq 2) as shown in Figures 1 and 2. Lateral approach of CH_2N_2 to **1-H** produces a stable bis-hydrazonato complex **3-H** (Me-in) with an overall exothermicity of −30.5 kcal/mol, only 12 kcal/mol less than the first insertion reaction (see Table 1). Similarly central insertion to **2-H** results in the Me-out bis-hydrazonato complex **4-H** (Me-out) with a similar overall energy of reaction (−31.3 kcal/mol). In contrast to the first insertion reaction, however, much larger barriers are found for addition of the second CH_2N_2 reactant. The barrier for central approach (**cnt TST2**) is 20.8 kcal/mol, while the corresponding barrier for lateral approach (**lat TST2**) is 18.8 kcal/mol. While significantly higher, these barriers would be prohibitive to formation of bis-hydrazonato complexes.

Comparing to the results using the bulkier $Ph_2C{=}N{=}N$ reactant (Figure 3 and Table 1), no major changes are apparent from the reaction profile. For example, for lateral approach the barrier height is 25 kcal/mol and the overall reaction energy is −24 kcal/mol (−23 kcal/mol when solvent effects are included) to produce **3-Ph** (Me-in).

In considering the structures of the products and transition states for this reaction (Figure 6) we note that the $Zr{-}N_1$ bond

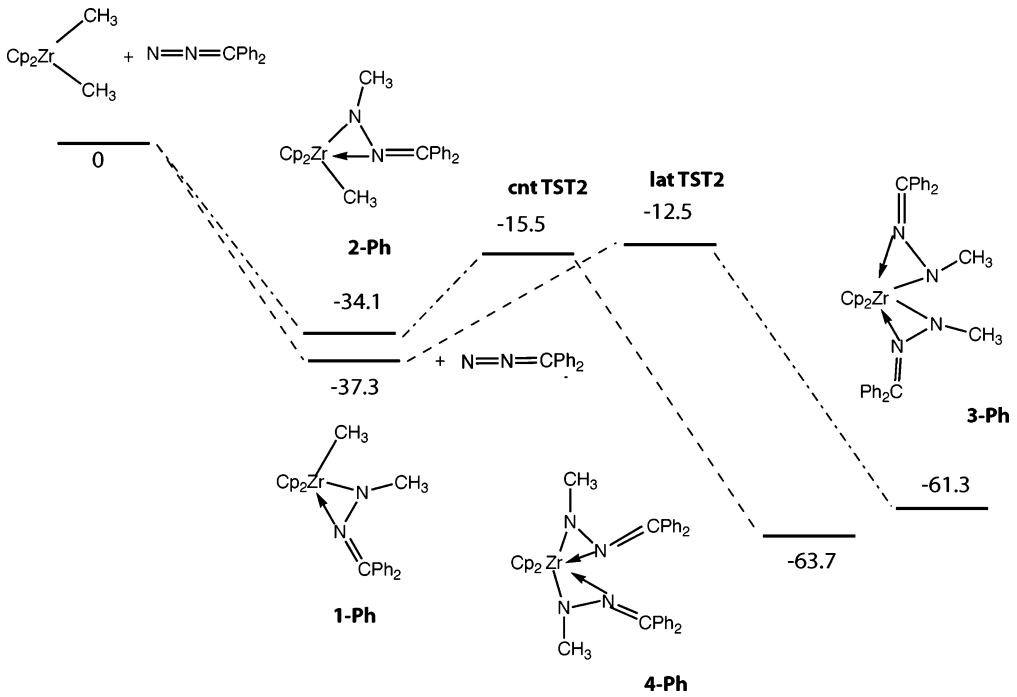

Figure 3. Reaction path of $Ph_2C{=}N{=}N$ addition to Cp_2ZrMe_2.

Table 1. Energies of Insertion Products of CR_2N_2 with Cp_2ZrMe_2 (results include zero-point energy corrections)

	relative energies (kcal/mol)		
	R = H	R = Ph	R = Ph
	gas phase	gas phase	toluene solvent
First Central Insertion			
$Cp_2ZrMe_2 + CR_2N_2$	0.0	0.0	0.0
adduct	−0.6		
cnt TST1	2.0		
2 $Cp_2ZrMe(hyd)$	−40.3	−34.1	−33.4
First Lateral Insertion			
$Cp_2ZrMe_2 + CR_2N_2$	0.0	0.0	0.0
lat TST1	7.7		
1 $Cp_2ZrMe(hyd)$	−42.1	−37.3	−36.4
Second Central Insertion			
2 $+ CR_2N_2$	0.0	0.0	0.0
cnt TST2	18.7	16.6	17.4
4 $Cp_2Zr(hyd)_2$	−31.3	−29.6	−28.3
Second Lateral Reaction			
1 $+ CR_2N_2$	0.0	0.0	0.0
lat TST2	20.1	24.8	24.8
3 $Cp_2Zr(hyd)_2$	−30.5	−24.0	−23.1

Table 2. Structural Parameters for $Cp_2ZrMe(Me{-}N{-}N{=}CR_2)$

	1-H (calc)	**1-Ph** (calc)	**1-Ph** (expt)[a]
$R(Zr{-}N_1)$, Å	2.162	2.142	2.103
$R(Zr{-}N_2)$, Å	2.307	2.338	2.283
$R(N_1{-}N_2)$, Å	1.347	1.350	1.338
$R(N{=}CR_2)$, Å	1.300	1.317	1.307
$R(Zr{-}CH_3)$, Å	2.303	2.308	2.357
R(Zr−Cp-cnt), Å	2.321	2.324	2.236
	2.323	2.329	2.242
$\angle Cp_1{-}Zr{-}Cp_2$, deg	128.9	129.3	128.22

[a] Ref 15.

lengths are virtually the same as in the mono-hydrazonato species (2.16 Å for **1-H** and **3-H**, 2.14 Å for **1-Ph** and **3-Ph**). However, the $Zr{-}N_2$ bond lengths increase from 2.34 Å for **1-Ph** to 2.44−2.47 Å (**3-Ph** and **4-Ph**), and slightly smaller increases (0.08−0.09 Å) occur in **3-H** and **4-H**. This may reflect in part a geometric response to the presence of four N lone pairs in this formally 20-electron species (see Electronic Structure section below).

The methyl group and η^2-NN atoms were nearly coplanar in **1-H** and **2-H**. While the respective Zr−NN planes remain relatively planar in the Me-out species **4-H**, the hydrazonato ligands are twisted considerably away from coplanarity in **3-H**. In both products **3-Ph** and **4-Ph** with the bulkier Ph groups (Figure 7) similar twisting is also observed.

Finally we note that a total of four possible products could arise from the second insertion step, and we have examined only two of the four possibilities. The other two involve the cross-reaction of lateral approach to **3-Ph** and central approach to **4-Ph**, but these intermediates were not pursued in this study.

To determine the dependence of the preceding results on the choice of density functional or basis set, the relative energies of the reactions involving CH_2N_2 were computed in the more accurate BS2 basis with B3LYP and PBE functionals as well as traditional MP2 theory. The results are summarized in Table 3. Only slight variations in the thermochemistry were evident for the PBE functional compared to B3LYP with the notable reduction in the predicted activation barrier (14 vs 21 kcal/mol) for the second insertion step. A similar barrier for this step was obtained with MP2, but a somewhat larger exothermicity was computed.

Discussion

The preceding results show that the bis-hydrazonato Zr complexes arising from reaction with $H_2C{=}N{=}N$ (3-H and 4-H) and $Ph_2C{=}N{=}N$ (3-Ph and 4-Ph), respectively, correspond to stable species. This raises two issues. The first concerns the relative stability of the formally 20-valence electron bis-hydrazonato species, if one treats the dinitrogen ligands each as a four-electron donor. The second raises the question as to why these species have not been isolated synthetically. To explore these issues in more detail, the electronic structure of the bis-hydrazonato species is analyzed in the following section. In the subsequent section electronic properties of the ligands are varied in a manner to explore possible stabilization strategies for these species.

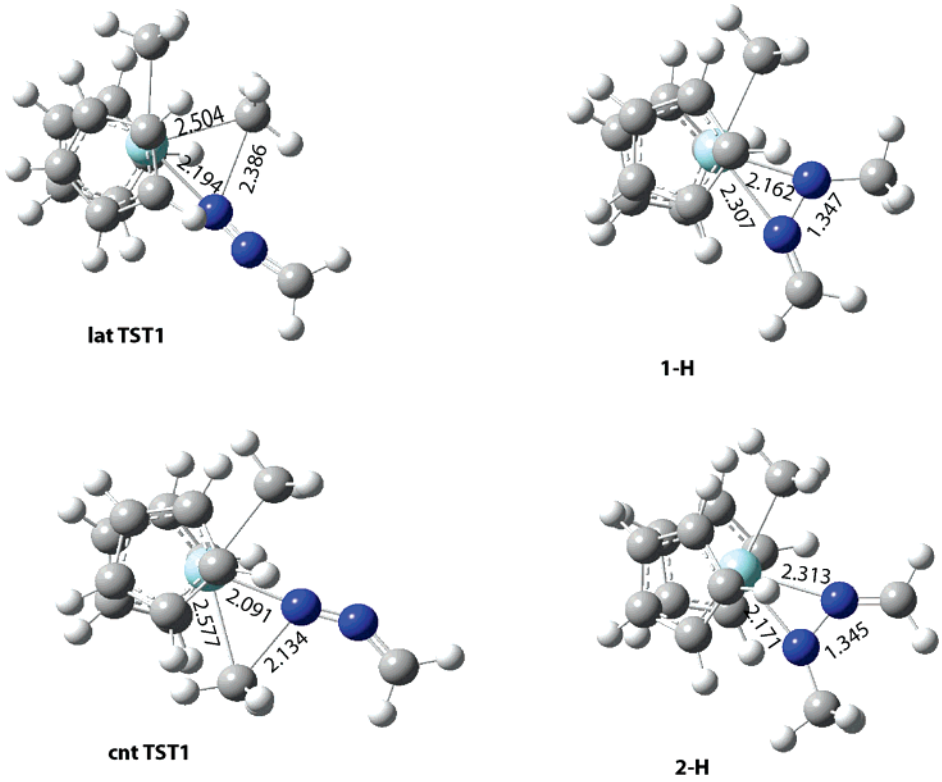

Figure 4. Structures of intermediates along first addition of $H_2C{=}N{=}N$ to Cp_2ZrMe_2.

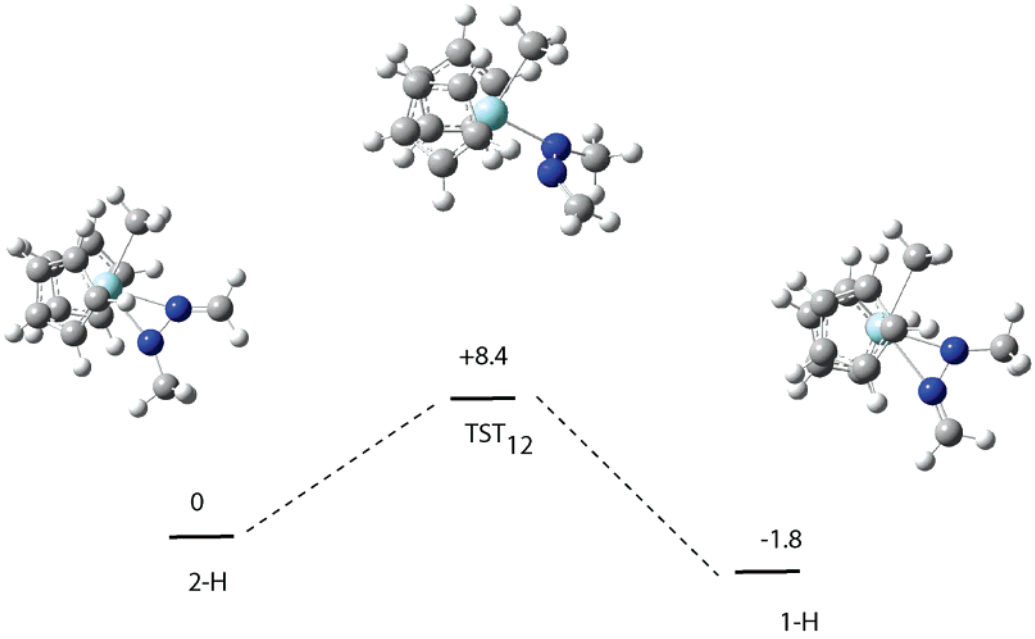

Figure 5. Intermediate for interconversion of **1-H** (Me-in) and **2-H** (Me-out).

Electronic Structure. Considering the electronic structure of **3-H** and **4-H**, each hydrazonato ligand has two N lone pairs (σ_1, σ_2) in addition to four electrons in the π system comprising a N π lone pair(π_1) and the C═N bond (π_2). In the bis-hydrazonato complexes the relevant bonding orbitals are four orbitals arising from the (σ_1, σ_2) lone pairs and two orbitals derived from the higher energy π_2 orbital. These orbitals are depicted for the **3-H** complex in Figure 8.

An analysis of the parentage of these six frontier orbitals in **3-H** and **4-H** is given in Table 4. In addition to these hydrazonato-based orbitals, the four π(Cp) orbitals arising from the e_1 set of the Cp ligands also lie in this energy region. The π_2(hyd) orbitals do not play a significant role in metal−ligand bonding, as shown by very small Zr admixtures in Table 4. There is significant 4d character (6 to 15%) in the four σ_1(hyd) and σ_2(hyd) orbitals that remain primarily localized on the N ligands. Regarding the role of these σ orbitals in the 20-valence-electron system, from an electronic point of view they are all stable MOs (Table 4). From a structural standpoint one notes the geometric distortions described above as the Zr−N_2 bonds lengthen by ∼0.1 Å between **1-Ph** and **3-Ph**, reflecting perhaps something less than two formal dative bonds.

Thermodynamic Stability. Returning to the nonexistence of the bis-hydrazonato species, we note that the vibrational

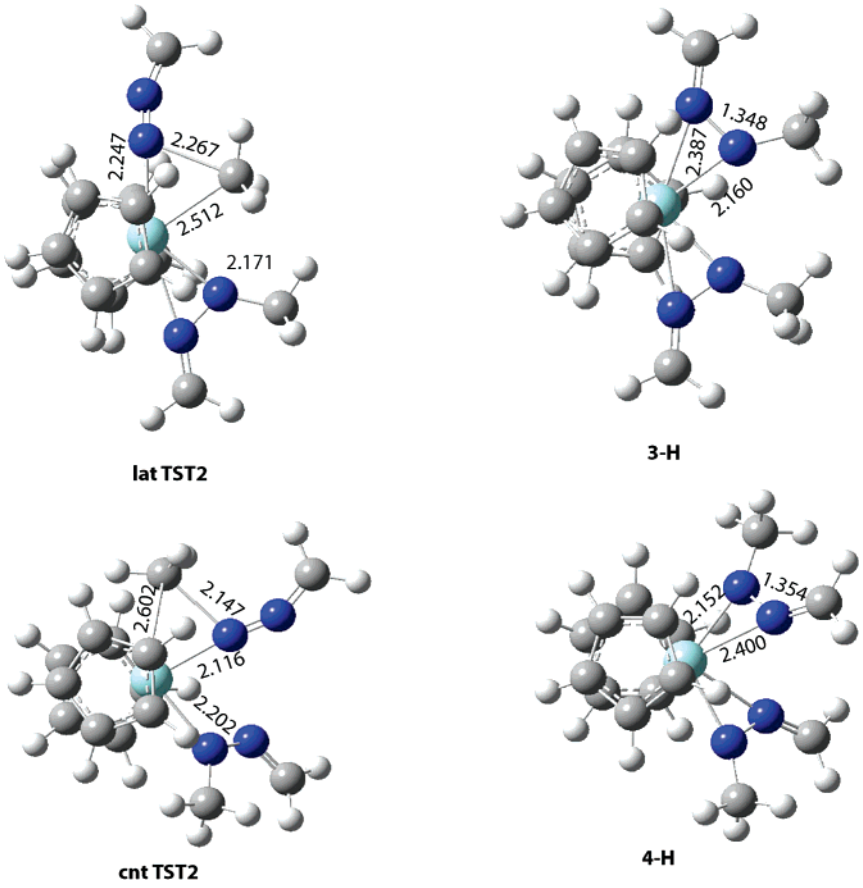

Figure 6. Structures of intermediates along second addition of $H_2C{=}N{=}N$ to Cp_2ZrMe_2.

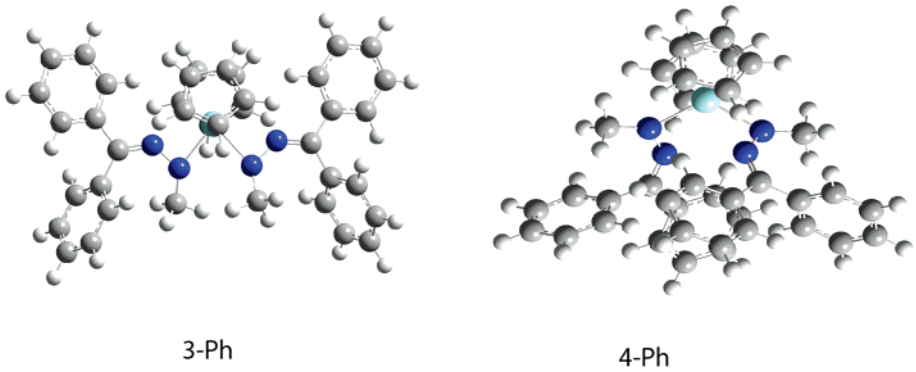

Figure 7. Structures of **3-Ph** and **4-Ph**.

Table 3. Comparison of Energies (kcal/mol) Involving Insertion of CH_2N_2 with Cp_2ZrMe_2 along the Central Path Using the Basis Sets BS1 and BS2 (results do not include ZPE corrections)

	B3LYP(BS1)	B3LYP(BS2)	PBE(BS2)	MP2(BS2)
First Central Insertion				
Cp_2ZrMe_2 + $H_2C{=}N{=}N$	0.0	0.0	0.0	0.0
2-H	−45.4	−43.7	−46.1	−52.2
Second Central Insertion				
2-H + $H_2C{=}N{=}N$	0.0	0.0	0.0	0.0
Cnt TST2	17.1	20.6	14.1	21.4
4-H	−34.6	−33.4	−34.6	−39.3

analysis of the realistic complexes **3-Ph** and **4-Ph** shows them to be stable species and viable synthetic targets. Thermodynamically their formation is predicted to be significantly exothermic relative to the mono-hydrazonato species from the single insertion reaction (see further discussion in Details of Calculation section). There are significant, but not prohibitive, barriers of 17−25 kcal/mol for the second insertion reaction to form these products.

As noted in the Introduction the bis-hydrazonato complexes have been isolated for actinide metals such as uranium, in contrast to the nonexistence for Zr or other transition metals. The role of 5f orbitals in the bonding is one important factor in the case of actinides. Another consideration is the role of ionic contributions to the bonding as the electronegativity of the ligand is varied. Regarding the latter possibility, two sets of model complexes are examined with more emphasis on the effects of electronegativities than on realistic prospects of synthesizing such species. Both Ph groups in the hydrazonato complexes, as in **3-Ph** $Cp_2Zr(CH_3{-}N{-}N{=}CPh_2)_2$, are replaced by increasingly more electronegative monofluoro and perfluoro groups denoted **3-Ph-F** and **3-Ph-F_5**. The resulting thermochemistries derived from optimized structures are summarized

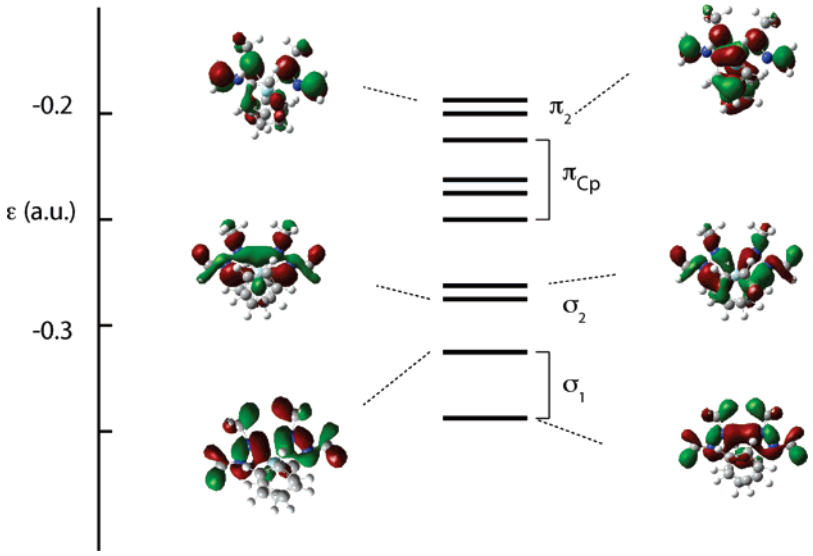

Figure 8. Frontier MOs for $Cp_2Zr(CH_3-N-N=CH_2)_2$ **3-H** (Me-in).

Table 4. Population Analysis of Molecular Orbitals in Two Isomers of $Cp_2Zr(CH_3-N-N=CH_2)_2$ (populations do not add to 100% since not all atoms or groups are tablulated)

			Population of MO (percent)					
MO	energy (au)	type	Zr 4d	N(hyd_A)	C(hyd_A)	N(hyd_B)	C(hyd_B)	Cp
3-H								
72	−0.191	π_2 (hyd)	0.3	14.7	9.1	14.5	8.9	22.2
71	−0.197	π_2 (hyd)	0.0	24.0	15.3	24.2	14.2	17.4
70	−0.203	π (Cp)	0.4	8.8	1.5	8.8	1.4	75.4
69	−0.233	π (Cp)	17.8	3.0	7.4	2.2	6.0	62.8
68	−0.234	π (Cp)	13.5	10.3	8.7	11.2	10.1	40.9
67	−0.242	π (Cp)	10.9	1.3	0.0	1.3	0.0	80.2
66	−0.283	σ_2 (hyd)	10.2	24.3	6.1	27.5	5.7	16.1
65	−0.286	σ_2 (hyd)	15.0	30.7	7.5	27.7	6.7	2.8
64	−0.316	σ_1 (hyd)	7.3	29.7	5.9	29.8	5.9	0.2
63	−0.335	σ_1 (hyd)	5.7	26.5	6.0	26.3	6.0	8.6
4-H								
72	−0.192	π_2 (hyd)	0.5	11.8	6.2	16.3	18.9	52.8
71	−0.195	π_2 (hyd)	0.8	23.0	13.4	17.7	10.6	46.5
70	−0.202	π (Cp)	2.0	17.5	9.7	17.1	9.4	39.6
69	−0.234	π (Cp)	8.1	1.3	1.4	1.7	1.8	79.6
68	−0.237	π (Cp)	17.4	6.9	7.5	6.9	7.2	62.1
67	−0.250	π (Cp)	16.5	0.9	0.0	1.0	0.0	77.4
66	−0.269	σ_2 (hyd)	10.1	27.3	6.0	29.9	7.6	7.8
65	−0.285	σ_2 (hyd)	10.2	29.7	6.9	27.1	6.5	6.7
64	−0.318	σ_1 (hyd)	6.4	30.5	5.8	30.3	5.8	0.7
63	−0.331	σ_1 (hyd)	8.5	25.9	6.4	25.9	6.4	7.0

Table 5. Comparison of Reaction Energies Forming Mono- and Bis-hydrazonato Zr Complexes $Cp_2Zr(CH_3)$(hyd) and $Cp_2Zr(hyd)_2$, Where Hyd = ($Me-N-N=CR_2$) and R = Ph, F−Ph, or F_5−Ph (product for each reaction is indicated in parentheses)

	reaction energies (kcal/mol)		
	R = Ph	R = F−Ph	R = F_5−Ph
Central Pathway (Me-out)			
first insertion, eq 1	−38.3 (**2-Ph**)	−39.2 (**2-Ph−F**)	−46.3 (**2-Ph−F_5**)
second insertion, eq 2	−33.0 (**4-Ph**)	−34.5 (**4-Ph−F**)	−29.6 (**4-Ph−F_5**)
sum, both insertions	−71.3	−73.7	−75.9
Lateral Pathway (Me-in)			
first insertion	−41.7 (**1-Ph**)	−42.2 (**1-Ph−F**)	−46.6 (**1-Ph−F_5**)
second insertion	−27.0 (**3-Ph**)	−28.0 (**3-Ph−F**)	−32.8 (**3-Ph−F_5**)
sum, both insertions	−68.7	−70.2	−79.4

in Table 5. The effects are particularly notable for the Me-in isomers where the bulky fluorophenyl groups are not in as close contact. For the first insertion one finds the reaction energy corresponding to the first insertion product to be more exothermic by 1 kcal/mol (**1-Ph-F**) and 5 kcal/mol (**1-Ph-F_5**). Nearly identical changes are also calculated for the reaction energies for the second insertion products **3-Ph-F** and **3-Ph-F_5**. Relative to the starting reactants (Table 5), the overall exothermicity of formation of the bis-hydrazonato complexes from initial reactants has increased in magnitude from −68.7 kcal/mol (**3-Ph**) to −70.2 kcal/mol (**3-Ph-F**) and −79.4 kcal/mol (**3-Ph-F_5**). While this study employed rather artificial models, these results nonetheless suggest that alterations of the ligands with enhanced electronegativity could increase the prospects of isolating these formally 20-valence-electron complexes.

Conclusions

The insertion of diazomethane reactants $R_2C{=}N{=}N$ (R = H, Ph) into the Zr−Me bonds of Cp_2ZrMe_2 has been examined using density functional techniques. The formation of the first insertion product $Cp_2Zr(CH_3)(CH_3{-}N{-}N{=}CR_2)$ proceeds to form the thermodynamically preferred isomer (**1-H** and **1-Ph**). The calculated and experimental structural features for this known species are in good agreement with the observed structure of the known complex **1-Ph**. Formation of this first insertion product is calculated to be −37.3 kcal/mol in the gas phase including zero-point energy corrections and −36.4 kcal/mol with solvent contributions in toluene (Table 1). The second insertion with **1-Ph** to form the unobserved bis-hydrazonato species **3-Ph** is predicted to proceed with a barrier of 25 kcal/mol and an exothermicity of −24 kcal/mol (−23 kcal/mol in toluene). Using values from enthalpies at 298 K instead gives similar results within 1 kcal/mol (see Supporting Information).

The electronic structure of these formally 20-valence-electron species shows significant Zr 4d admixture in the σ bonds involving the nitrogen ligands and four stable MOs corresponding to the N lone pairs. There is some structural distortion between the mono- and bis-hydrazonato species. While the "covalent" $Zr{-}N_1$ bond remains essentially unchanged at 2.14 Å in both mono- and bis-hydrazonato species, the second "dative" $Zr{-}N_2$ bond lengths increase substantially from 2.338 Å in the first insertion product (**1-Ph**) to 2.469 Å (**3-Ph**) and 2.442 Å (**4-Ph**) in the second insertion product.

Acknowledgment. The author thanks Dr. Jaqueline Kiplinger for collaborations involving experimental studies of actinide hydrazonato complexes and other organoactinide compounds in recent years that stimulated these investigations. This work was supported by the Heavy Element Chemistry program at Los Alamos National Laboratory under the auspices of the National Nuclear Security Administration of the U.S. Department of Energy under Contract No. DE-AC52-06NA25396.

Supporting Information Available: Calculated thermochemical properties and Cartesian coordinates for calculated structures. This material is available free of charge via the Internet at http://pubs.acs.org.

OM070107W